New Materials, Compounds and Applications
Vol.6, No.1, 2022, pp.37-43

PHASE RELATIONS IN THE $CuSbS_2$-Sb_2S_3-Sb SYSTEM

P.R. Mammadli[1,2,3*], V.A. Gasimov[3], L.F. Mashadiyeva[3], D.M. Babanly[1,3]

[1]Azerbaijan State Oil and Industry University, Baku, Azerbaijan
[2]French -Azerbaijani University (UFAZ), Baku, Azerbaijan
[2]Nagiyev Institute of Catalysis and Inorganic Chemistry of ANAS, Baku, Azerbaijan

Abstract. Phase relations in the $CuSbS_2$-Sb_2S_3-Sb system were determined experimentally over the entire concentration range by means of differential thermal analysis (DTA) and powder x-ray diffraction (PXRD) techniques. One boundary, two internal polythermal sections, and the liquidus surface projection of the system were constructed. Primary crystallization fields of existing phases, as well as, types and coordinates of non- and monovariant equilibria were determined. It was defined that, the concentration triangle under study is an independent subsystem of the Cu-Sb-S ternary system and belongs to the monotectic type with a wide stratification field of two liquids.

Keywords: *DTA, PXRD, phase diagram, stibnite, chalcostibite, immiscibility field.*

Corresponding Author: *Parvin Mammadli, Azerbaijan State Oil and Industry University; French - Azerbaijani University (UFAZ), Nizami str. 183, Baku, Azerbaijan, e-mail: parvin.mammadli@ufaz.az*

Received: *7 December 2021;* ***Accepted:*** *16 February 2022;* ***Published:*** *19 April 2022.*

1. Introduction

Research in the preparation of less-toxic, earth-abundant functional materials is highly pursued in order to decrease the cost for the possibility at large scales manufactures. In this regard, considerable research attention has been focused on the application of binary and ternary copper-antimony chalcogenides as non-toxic, easily available materials with possessing properties and a wide range of applications including solar cells, sensors, absorbers, thermoelectric devices, field-effect transistors, etc. (Suehiro *et al.*, 2015; Peccerillo & Durose, 2018; Krishnan *et al.*, 2015).

Antimony sulfide (Sb_2S_3) is considered a popular photovoltaic candidate for thin-film solar cells due to its high absorption coefficient, single stable phase, and benign synthesis conditions (Kondrotas *et al.*, 2018; Ishaq *et al.*, 2020). Ternary chalcostibite - copper antimony sulfide ($CuSbS_2$) has been proposed as an emerging semiconductor material having interesting optoelectronic and photovoltaic properties due to its appropriate bandgap, high absorption coefficient, and hole mobility (Vinayakumar *et al.*, 2018; Yang *et al.*, 2014; Rabinal & Mulla, 2019).

One of the main approaches to the development of new advanced materials in inorganic materials science is the study of phase diagrams composed of known phases with interesting functional properties (Babanly *et al.*, 2017, 2019; Babanly & Tagiyev, 2018). In our previous studies, considering the scientific and practical importance of the Cu-Sb-S ternary system in terms of the search for environmentally friendly, low-cost functional materials, the solid-phase equilibrium diagram of this system, and the thermodynamic properties of copper antimony sulfides were studied (Mashadiyeva *et al.*, 2021). Later on, the CuSbS2-Cu_3SbS_3-Sb_2S_3 concentration triangle of this system

was studied in (Mammadli *et al.*, 2021).

In the present contribution, as a continuation of our investigations, we report about the phase relations in the subsystem $CuSbS_2$-Sb_2S_3-Sb (A).

Constituent phases of the subsystem (A) have been studied in detail. Sb_2S_3 (stibnite) melts congruently at 823 K (Massalski *et al.*, 1990) and crystallizes into orthorhombic structure with the space group P*nma*: *a* = 11.3107; *b* = 11.2285 Å; *c* = 3,8363 (Bayliss & Nowacki, 1972). $CuSbS_2$ ternary compound is reflected in the phase diagram of the Cu_2S-Sb_2S_3 system (Cambi & Elli, 1965; Kuliyev *et al.*, 1969; Babanly *et al.*, 1993). It melts congruently at 828 K (Babanly *et al.*, 1993) and crystallizes into the orthorhombic structure (Sp.gr. P*nma*): *a* = 6.018(1), *b* = 3.7958(6), and *c* = 14.495(7) Å (Kyono & Kimata, 2005; McCarthy *et al.*, 2016).

Two boundary quasi-binary constituents of the system A have been studied in detail. The system Sb_2S_3-S is characterized by the monotectic and eutectic equilibria (Massalski *et al.*, 1990). The phase diagram of the system $CuSbS_2$ - Sb_2S_3 is of a simple eutectic type (Babanly *et al.*, 1993).

2. Experimental part

Alloys of the system $CuSbS_2$-Sb_2S_3-Sb (A) were prepared from the preliminarily synthesized and identified Sb_2S_3, $CuSbS_2$ compounds, and elemental sulphur. Elemental copper (Cu-00029; 99.9999%), antimony (Sb-00002; 99.999%) and sulphur (S -00001; 99.999%) of high purity from *Evochem Advanced Materials GmbH* (Germany) were used for synthesis.

Compounds were synthesized by fusion of the elemental substances in stoichiometric ratios in evacuated up to ~10^{-2} Pa and sealed quartz ampoule of the 15x1.5 cm size in a two-zone inclined furnace (Mashadiyeva et al., 2021; Mammadli et al., 2021). The temperature of the hot zone of the furnace was gradually increased to ~50^0C higher than the melting point of the corresponding compound within 3-4 hours, while the temperature of the upper, "cold" zone of the furnace was 650 K, which is slightly below the boiling point of sulphur (718 K (Emsley, 1998)). The synthesis was continued in this mode for the next 3-4 hours and the ampoules were completely transferred into the hot zone. The resulting liquids were mixed by shaking the alloys and the oven was gradually cooled. After synthesis, the ampoules were kept at 750 K for 100 h.

Identity of the synthesized compounds was monitored by differential thermal analysis (DTA) and powder X-ray diffraction (PXRD) methods, obtained data well coincided with the literature (Massalski *et al.*, 1990; Bayliss & Nowacki, 1972; Cambi & Elli, 1965; Kuliyev *et al.*, 1969; Babanly *et al.*, 1993; Kyono & Kimata, 2005; McCarthy *et al.*, 2016).

Two sets of samples (0.5 g by mass each) were prepared by co-melting of different proportions of the preliminarily synthesized compounds in evacuated quartz ampoules. After melting, alloys were annealed at about ~40-50^0 below the solidus temperature for ~1000 hours in order to get completely homogenized samples.

Obtained equilibrium samples were examined by DTA and PXRD methods. DTA of the samples was carried out in evacuated quartz ampoules on a differential scanning calorimeter of the 404 F1 Pegasus System (NETZSCH). NETZSCH Proteus Software was used to process the results of measurements. The accuracy of the temperature measurements was within $\pm 2^0$. X-ray analysis was carried out at room temperature on

the Bruker D2 PHASER diffractometer with $CuK\alpha_1$ radiation. Topas 4.2 Software was used to index obtained diffraction patterns.

3. Results and discussion

On the phase diagram of the system (A) and its various sections, the compositions of alloys are expressed in equal numbers of atoms using the corresponding coefficients in front of their formulas. This is identical to the expression of composition in atomic percent and allows this data to be used in the general phase diagram of the Cu-Sb-S system without recalculation of composition.

3.1. $CuSbS_2$ – Sb quasi-binary system

As it can be seen from the T-x diagram constructed based on the DTA results (Fig.1), the system $CuSbS_2$ – Sb is of monotectic type. Monotectic equilibrium

$L_1 \leftrightarrow L_2 + Sb$

is established at 880K. The immiscibility area at this temperature (mm′ horizontal line) occupies 10-87 at% elemental antimony concentration interval.

$L \leftrightarrow CuSbS_2 + Sb$

eutectic equilibrium € has ~5 at. % Sb (elem.) composition and crystallizes at 818K.

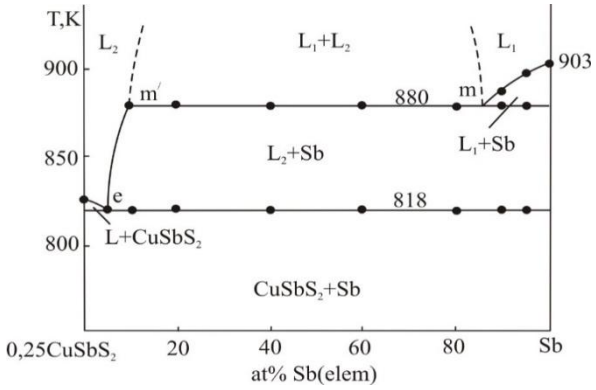

Figure 1. The T-x phase diagram of the system $CuSbS_2$-Sb

XRD results show that alloys of the system under study are composed of $CuSbS_2$ + Sb two-phase mixture (Fig.2). As can be seen from Fig.2, these diffraction patterns are composed of the diffraction lines of $CuSbS_2$ and elemental antimony.

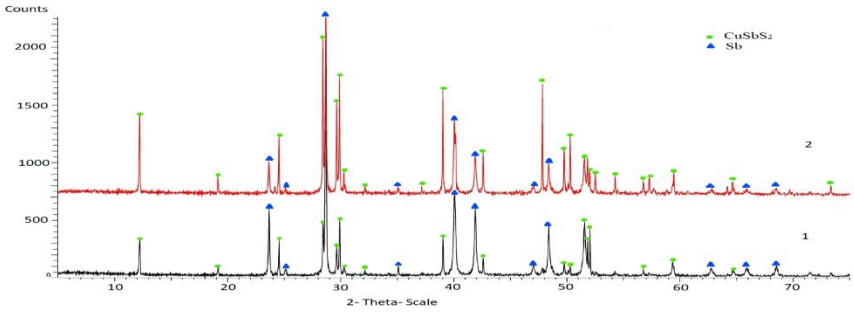

Figure 2. PXRD spectrum of the two alloys of the $CuSbS_2$-Sb system: 1- 20 mol% $CuSbS_2$ + 80 mol% Sb; 2- 50 mol% $CuSbS_2$ + 50 mol% Sb

3.2. Projection of the liquidus surface (Fig. 3)

The projection of the liquidus surface of the system A on the concentration triangle is given in Fig. 3. It is obvious that the concentration triangle $CuSbS_2$-Sb_2S_3-Sb is an independent subsystem and characterized by eutectic and monotectic equilibriums. There is a stratification field of two liquids ($m_1m_2m_2'm_1'$) in a wide concentration interval. This immiscibility field is located in the primary crystallization area of the elemental antimony and divides it into 2 parts (areas 1 and 2). Elemental antimony crystallizes from the liquid rich in elemental antimony (L_1) in the area 1 and from the liquid based on sulfides (L_2) in the area 2. Primary crystallization areas of the Sb_2S_3 and $CuSbS_2$ phases (areas 3 and 4) exist in the form of two thin strips along the $CuSbS_2$-Sb_2S_3 boundary system.

Liquidus surfaces of phases are bordered by the e_1E, e_2E and e_3E eutectic curves (Fig.3):

e_1E curve: $L \leftrightarrow CuSbS_2 + Sb$ T=818-750K (1)

e_2E curve: $L \leftrightarrow CuSbS_2 + Sb_2S_3$ T=765-750K (2)

e_3E curve: $L \leftrightarrow Sb_2S_3 + Sb$ T=793-750K (3)

These curves converge in the triple eutectic point E:

$L \leftrightarrow CuSbS_2 + Sb_2S_3 + Sb$ T=750K (4)

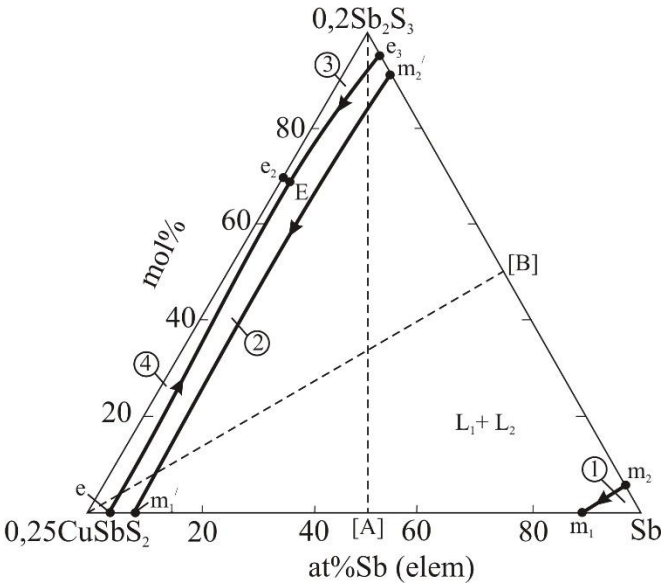

Figure 3. Projection of the liquidus surface of the system $CuSbS_2$-Sb_2S_3-Sb. Primary crystallization fields: 1,2 – Sb, 3 – Sb_2S_3, 4 – $CuSbS_2$. Dotted lines are studied polythermal sections

Non- and monovariant equilibria of the system are given in the table.

Table. Non- and monovariant equilibria in the system $CuSbS_2$-Sb_2S_3-Sb

Point or curve in the Fig.3	Equilibria	Temperature, K
e_1	$L \leftrightarrow CuSbS_2 + Sb$	818
e_2	$L \leftrightarrow CuSbS_2 + Sb_2S_3$	765
e_3	$L \leftrightarrow Sb_2S_3 + Sb$	793
E	$L \leftrightarrow CuSbS_2 + Sb_2S_3 + Sb$	750
$m_1(m_1')$	$L_1 \leftrightarrow L_2 + Sb$	880
$m_2(m_2')$	$L_1 \leftrightarrow L_2 + Sb$	888
e_1E	$L \leftrightarrow CuSbS_2 + Sb$	815-750
e_2E	$L \leftrightarrow CuSbS_2 + Sb_2S_3$	765-750
e_3E	$L \leftrightarrow Sb_2S_3 + Sb$	793-750
m_2m_1 (m_2' m_1')	$L_1 \leftrightarrow L_2 + Sb$	888-880

3.3. Polythermal sections (Fig.4 a,b)

Two polythermal sections of the phase diagram of the system A are given below (Fig.4 a,b) and analyzed in context with the projection of the liquidus surface (Fig.3). Here, [A] and [B] are 1:1 mix ratios of the constituent substances of the $0.25CuSbS_2$-Sb and $0.2Sb_2S_3$-Sb boundary binary systems, consequently.

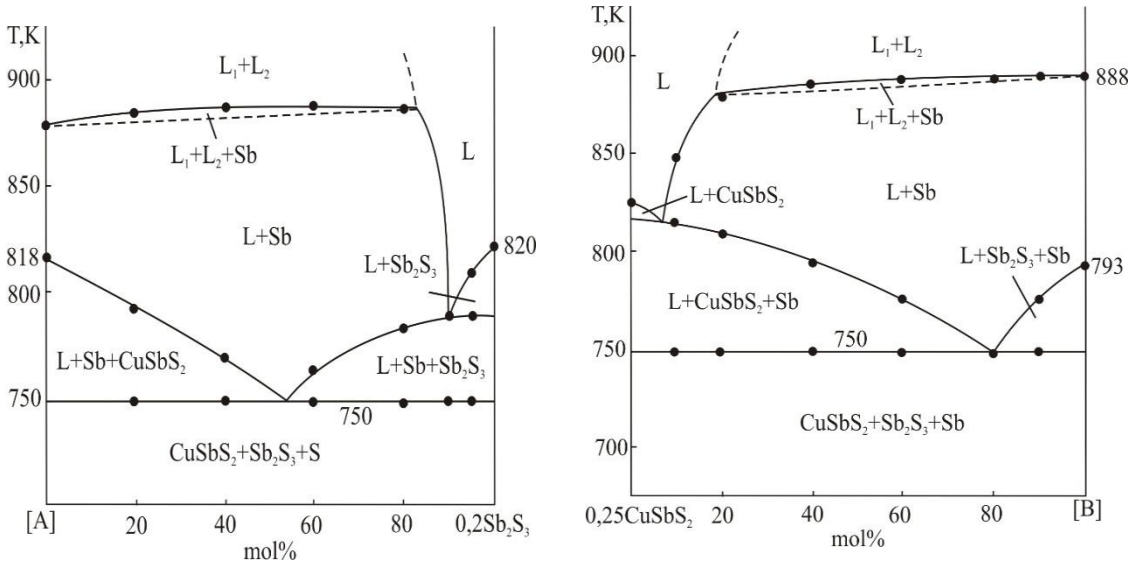

Figure 4. T-x phase diagrams of the systems $0.2Sb_2S_3$- [A] (a) and 0.25 $CuSbS_2$ – [B] (b)

0.2 Sb_2S_3- [A] polythermal section (Fig.4a)

There is a wide (~ 80 mol%) immiscibility region of two liquid phases along this polythermal section. Elemental antimony crystallizes by $L_1 \leftrightarrow L_2 + Sb$ monovariant monotectic reaction within this area. Since this reaction occurs in a very small ($3\text{-}4^0$C) temperature interval, on DTA curves thermal effects belonging to them form sharp peaks as in isothermic melting. Therefore, the $L_1 + L_2 + Sb$ three-phase area reflecting those monovariant processes are indicated by dotted lines on the T-x diagram (Fig.4a).

Sb_2S_3 is primarily crystallized from the area rich in Sb_2S_3 (>90 mol%). Below the liquidus curve, from left to the right, crystallization continues by the e_1E and e_3E monovariant eutectic schemes and ends by the crystallization of the ternary eutectics E at 750K.

0.25 $CuSbS_2$ – [B] polythermal section (Fig.4b)

Crystallization processes along this polythermal section are qualitatively similar to the ones in the previous system. The only difference is that here initial crystallization of the $CuSbS_2$ compound takes place in a small (~ 5 mol%) concentration interval (Fig.4b).

Thus, a comparative analysis of all elements of the phase diagram (Fig. 1,3,4) indicates their compatibility with each other. Presented results can be used to prepare phases based on the primary constituents of the system A, as well as and their eutectic composites.

4. Conclusion

For the first time, the nature of the physicochemical interaction of the stibnite, chalcostibite minerals, and elemental antimony was determined using DTA and powder X-ray methods. The phase diagram of the $CuSbS_2$ – Sb boundary system, 2 isopleth sections, as well as, the surface of the liquidus surface of the $CuSbS_2$-Sb_2S_3-Sb system were constructed. It was established that the system is of eutectic and monotectic type and characterized by the formation of a wide immiscibility area L_1+L_2 of two liquid phases.

Acknowledgment

The work has been partially supported by the Science Development Foundation under the President of the Republic of Azerbaijan, a grant № EİF-BGM-4-RFTF-1/2017-21/11/4-M-12.

On behalf of all authors, the corresponding author states that there is no conflict of interest.

References

Babanly, D.M., & Tagiyev, D.B. (2018). Physicochemical aspects of ternary and complex phases development based on thallium chalcohalides. *Chem. Probl., 16*(2), 153-177.

Babanly, M.B., Chulkov, E.V., Aliev, Z.S., Shevelkov, A.V., & Amiraslanov, I.R. (2017). Phase diagrams in materials science of topological insulators based on metal chalcogenides. *Russ. J. Inorg. Chem., 62*(13), 1703–1729.

Babanly, M.B., Mashadiyeva, L.F., Babanly, D.M., Imamaliyeva, S.Z., Tagiev, D.B., & Yusibov, Yu.A. (2019). Some issues of complex studies of phase equilibria and thermodynamic properties in ternary chalcogenide systems involving EMF measurements (review). *Russ. J. Inorg. Chem., 64*(13), 1649-1671.

Babanly, M.B., Yusibov, Yu.A., & Abishev, V.T. (1993). *Three-Component Chalcogenides Based on Copper and Silver*, Baku: BSU, 342. (In Russian).

Bayliss, P. Nowacki, W. (1972). Refinement of the crystal structure of stibnite, Sb_2S_3. *Z. Kristallogr*., 135, 308-315.

Cambi, L. Elli, M. (1965). Processi idrotermali. Sintesi di solfosali da ossidi di metallic e metalloidi. *Chimica Industria., 47*(2), 136-147.

Emsley, J. (1998). *The Elements.* New York: Oxford University Press, 3rd ed., 300.

Ishaq, M., Chen, S., Farooq, U., Azam, M., Deng, H., Su, Z.-H., Zheng, Z.-H., Fan, P., Song, H.-S., & Liang, G.-X. (2020). High Open-Circuit Voltage in Full-Inorganic Sb_2S_3 Solar Cell via Modified Zn-Doped TiO_2 Electron Transport Layer. *Solar RRL, 4*(12), 2000551-2000575.

Kondrotas, R., Chen, C., & Tang, J. (2018). Sb_2S_3 Solar Cells. *Joule, 2*(5), 857–878.

Krishnan, B., Shaji, S., & Ernesto Ornelas, R. (2015). Progress in development of copper antimony sulfide thin films as an alternative material for solar energy harvesting. *J. Mater. Sci: Mater. Electron., 26*(7), 4770–4781.

Kuliyev, R.A., Krestovnikov, A.N., & Glazov, V.M. (1969). Enquire into phase equilibria between Cu and Sb chalcogenides. *Izv. An. SSSR, Inorganic Materials., 5*(12), 2217-2218.

Kyono, A. & Kimata, M. (2005). Crystal structures of chalcostibite ($CuSbS_2$) and emplectite ($CuBiS_2$): Structural relationship of stereochemical activity between chalcostibite and emplectite. *Am. Mineral., 90*(1), 162-165.

Mammadli, P.R., Mashadiyeva, L.F., Gasimov, V.A., Dashdiyeva, G.B., & Babanly, D.M. (2021). Phase Relations in the $CuSbS_2$-Cu_3SbS_4-Sb_2S_3 System. *AJCN, 3*(1), 100-108.

Mashadiyeva, L.F., Mammadli, P.R., Babanly, D.M., Ashirov, G.M., Shevelkov A.V., & Yusibov Y.A. (2021). Solid-Phase Equilibria in the Cu-Sb-S System and Thermodynamic Properties of Copper-Antimony Sulfides. *JOM., 73*(5), 1522–1530.

Massalski, T.B., Okamoto, H., Subramanian, P.R., & Kacprzak, L. (1990). Binary alloy phase diagrams. ASM International, 2nd ed., Materials Park, Ohio, USA, 3, 3589.

McCarthy, C.L., Cottingham, P., Abuyen, K., Schueller, E.C., Culver, S.P., & Brutchey, R.L. (2016) Earth-abundant $CuSbS_2$ thin films solution-processed from thiol–amine mixtures. *J. Mater. Chem. C., 4*(26), 6230-6233.

Peccerillo, E. Durose, K. (2018). Copper–antimony and copper–bismuth chalcogenides-Research opportunities and review for solar photovoltaics. *MRS Energy & Sustainability, 5*(9), 1-59.

Rabinal, M.H.K., Mulla, R. (2019). Copper Sulfides: Earth-Abundant and Low-Cost Thermoelectric Materials. *Energy Technol., 7*(7), 1800850-1800970.

Suehiro, S., Horita, K., Yuasa, M., Tanaka, T., Fujita, K., Ishiwata, Y., Shimanoe, K., & Kida, T. (2015). Synthesis of Copper–Antimony-Sulfide Nanocrystals for Solution-Processed Solar Cells. *Inorg. Chem., 54*(16), 7840–7845.

Vinayakumar, V., Shaji, S., Avellaneda, D., Aguilar-Martínez, J.A., & Krishnan, B. (2018). Copper antimony sulfide thin films for visible to near infrared photodetector applications. *RSC Adv., 8*(54), 31055–31065.

Yang, B., Wang, L., Han, J., Zhou, Y., Song, H., Chen, S., Zhong, J., Lv, L., Niu, D., & Tang, J. (2014). $CuSbS_2$ as a Promising Earth-Abundant Photovoltaic Absorber Material: A Combined Theoretical and Experimental Study. *Chem. Mater., 26*(10), 3135–3143.